



OPEN Characteristics of SARS-CoV-2 variants and potential co-infected pathogens in hospitalized patients based on metagenomic next-generation sequencing

Xinxin Li^{1,6}, Chenyue Tang^{1,6}, Min Zhou², Jianqing Mi³, Jialin Liu⁴, Lizhong Han⁵, Xiaoqi Yu^{1,7}✉ & Xinxin Zhang^{1,7}✉

Metagenomic next-generation sequencing (mNGS) is widely used to diagnose complex infections in hospitalized patients, particularly those associated with COVID-19 which has garnered significant concern over the past five years. To investigate the molecular epidemic of the viral variant and the potential co-infection pathogens, we conducted retrospective mNGS analysis of 254 SARS-CoV-2-positive specimens collected from 200 hospitalized patients between March and September 2023. Phylogenetic analysis of the identified Omicron subvariants showed minimal evolutionary divergence, with no association between sub-lineages and pneumonia severity. Notably, mNGS demonstrated enhanced detection of polymicrobial coinfections, identifying bacterial, fungal, and viral co-pathogens in 92.5% (185/200) of cases. Pneumonia severity was associated with advanced age (proportion of elderly patients: 61.1 vs 78.3%; $p = 0.032$) and comorbid conditions, particularly diabetes mellitus (OR 2.03, 95% CI 1.03–4.02, $p = 0.041$), but showed no correlation with SARS-CoV-2 sub-lineages or coinfecting pathogens. While mNGS enhances coinfection diagnosis, COVID-19 outcomes are predominantly driven by host factors rather than Omicron subvariant evolution. Prioritized monitoring of elderly and comorbid individuals remained critical for severe pneumonia management.

Keywords Metagenomic next-generation sequencing (mNGS), Co-infection, Severe pneumonia (SP), COVID-19

Abbreviations

mNGS	Metagenomic next-generation sequence
SARS-CoV-2	Severe acute respiratory syndrome coronavirus 2
SP	Severe pneumonia
SCAP	Severe community-acquired pneumonia
COVID-19	Coronavirus disease 2019
WBC	White blood cell
UMSI	Unique molecular sample index
BALF	Bronchoalveolar lavage fluid
NCBI	National center of biotechnology information
BWA	Burrows-Wheeler aligner
MAF	Minor allele frequency

¹Department of Infectious Diseases, Research Laboratory of Clinical Virology, Ruijin Hospital, Shanghai Jiao Tong University School of Medicine, No.197 Ruijin 2nd Road, Shanghai 200025, China. ²Department of Pulmonary and Critical Care Medicine, Ruijin Hospital, Shanghai Jiao Tong University School of Medicine, Shanghai, China. ³Shanghai Institute of Hematology, State Key Laboratory of Medical Genomics, National Research Center for Translational Medicine at Shanghai, Ruijin Hospital, Shanghai Jiao Tong University School of Medicine, Shanghai, China. ⁴Department of Geriatrics, Ruijin Hospital, Shanghai Jiao Tong University School of Medicine, Shanghai, China. ⁵Department of Laboratory Medicine, Ruijin Hospital, Shanghai Jiao Tong University School of Medicine, Shanghai, China. ⁶Xinxin Li and Chenyue Tang contributed equally to this work. ⁷Xiaoqi Yu and Xinxin Zhang jointly supervised this work. ✉email: yuxiaoqi_03@163.com; zhangx@shsmu.edu.cn

VEP	Variant effect predictor
HQM	High-quality mapped
IQR	Interquartile range
CI	Confidence interval
ECMO	Extracorporeal membrane oxygenation
TTV	Torque teno virus
EBV	Epstein-Barr virus
HHV-7	Human herpesvirus-7
HSV-1	Herpes simplex virus-1
CMV	Cytomegalovirus
HHV-6	Human herpesvirus-6
RV-A/C	Rhinovirus A/C
HCoV-OC43	Human coronavirus-OC43
HMPV	Human metapneumovirus
HRSV-B	Human respiratory syncytial virus B
VZV	Varicella zoster virus
ICU	Intensive care unit
VOC	Variant of concern
CNCB	China national center for bioinformatics

Metagenomic next-generation sequencing (mNGS), an efficient, high-throughput approach for pathogen detection, is increasingly used in clinical laboratories^{1,2}. It is particularly effective in identifying rare, novel, and hard-to-detect pathogens³. A prominent example is the rapid identification of SARS-CoV-2 within one week in the early breakout of coronavirus disease 2019 (COVID-19) pandemic using mNGS⁴. In addition to diagnosing infectious diseases, mNGS also performed well in phylogenetic analysis of SARS-CoV-2 compared to whole-genome sequencing⁵. Since its initial emergence, SARS-CoV-2 has evolved from the ancestral strain through multiple generations of Omicron subvariants⁶. As the persistent emergence of SARS-CoV-2 variants in recurrent waves, particularly frequent sequential reinfections with Omicron subvariants, necessitates updated vaccination strategies⁷, the evolution of virus and its clinical significance should be monitored^{8,9}.

SARS-CoV-2 often leads to co-infections secondary infections with bacteria, fungi, and other viruses¹⁰. Compared with traditional diagnostic methods such as real-time PCR, microbial culture, and antigen or antibody detection, mNGS can simultaneously detect all microorganisms present in a specimen^{11,12}. Combined diagnostic approaches with mNGS have resulted in a five-fold increase in the detection rate of the pathogens in adult patients with severe community-acquired pneumonia (SCAP), compared with only routine cultures¹³. Metagenomic next-generation sequencing has demonstrated established clinical utility in infection diagnosis and therapeutic regimen adjustment, particularly through its capability to comprehensively characterize polymicrobial infections^{14,15}.

In this study, we conducted a retrospective analysis to gain detailed insights into SARS-CoV-2 variants and potential co-infections in COVID-19 cases using metagenomic next-generation sequencing (mNGS) data collected over six months.

Material and methods

Study design and SARS-CoV-2 positive samples collection

A total of 5,686 samples were collected retrospectively from March to September 2023 in Ruijin Hospital Affiliated to Shanghai Jiaotong University School of Medicine, of which 254 (4.47%) were positive for SARS-CoV-2. Only one result was included for each patient. Fifty-four samples were excluded due to repeated patient sources (Fig. 1). Most samples were from respiratory tract specimens, including 116 sputum (58%), 42 bronchoalveolar lavage fluid (BALF) (21%), and 38 nasopharyngeal swabs (19%). Four patients tested positive for SARS-CoV-2 in blood, with no other types of samples collected from them.

Wet-lab pipelines for mNGS

We employed metagenome, meta-transcriptome and targeted metagenome to detect pathogen as previously described². All samples were centrifuged at 12,000 × g for 5 min to collect the pathogens and human cells. Next, 50 µL of precipitate was taken to deplete of host nucleic acid using 1 U of Benzonase (Sigma) and 0.5% Tween 20 (Sigma), incubated at 37 °C for 5 min. The reaction was stopped with 400 µL of a terminal buffer¹⁶. The unique molecular sample index (UMSI), composed of quantified DNA fragments, was spiked into each sample as a maker and internal control. The mixture (600µL) was triturated in new tubes with 500 µL of ceramic beads utilizing a Minilys personal TGrinder H24 homogenizer (Tiangen, China). Then, nucleic acid was extracted and eluted in 65 µL of elution buffer by QIAamp UCP pathogen minikit (Qiagen, Germany)². For RNA extraction and reverse transcription, 200 µL of the samples was extracted following manufacturer's instructions with QIAamp Viral RNA Mini Kit (Qiagen, Germany). cDNAs were generated using the QIAseq FastSelect -rRNA HMR Kit (Qiagen, Germany); Both DNA and cDNA were quantified using a Qubit double-stranded DNA (dsDNA) high-sensitivity (HS) assay kit (Invitrogen, USA). Indexed DNA libraries were constructed with a TruePrep DNA Library Prep Kit (Vazyme Biotech, China)^{17,18}. 4) An aliquot of 750 ng library from each sample was used for hybrid capture-based microbial probe¹⁹ enrichment through one round of hybridization (SeqCap EZ Library, Roche, USA). Library was quantified with a Qubit dsDNA HS Assay Kit and assessed using an Agilent 2100 Bioanalyzer and a High Sensitivity DNA Kit (Agilent Technologies, USA). Sequencing was performed with an Illumina NextSeq 550 sequencer (Illumina, USA) with 75-cycle single-end sequencing.

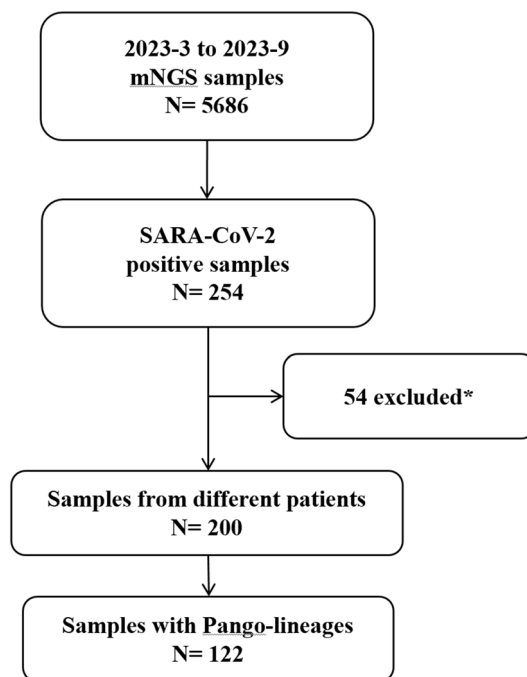


Fig. 1. The flowchart of sample and clinical data collection of COVID-19 patients. COVID-19 corona virus disease 2019. *Only one sample of each patient was enrolled.

Bioinformatics analyses for microorganism

Bioinformatics analyses were performed as previously described with adjusted details²⁰. Trimmomatic²¹ and K-complexity²² were employed to remove low quality and low complexity reads, adapter contamination, and duplicate reads, as well as those shorter than 40 bp. Human sequence data were discarded by mapping to a human reference genome (hg38) using Burrows-Wheeler Aligner software²³. The final database of representative assemblies of microorganisms and pathogen lists consisted of approximately 20,000 genomes²⁴. SNAP v1.0beta.18 (<https://github.com/amplab/snap>) was used to align the microbial reads. DNA or RNA viruses reported as positive required coverage of three or more non-overlapping regions on the genome. A species/genus-positive detection was defined when the reads per million (RPM) ratio, or RPM-r, was more than 5, where RPM-r was defined as the RPM in the clinical sample divided by the RPM in the negative control²⁵. Each finalized report was reviewed by two qualified medical technicians. The presence of co-infections was determined through a) potential pathogenicity assessment of detected pathogens at the sampling site; b) relevance to conventional laboratory results; c) final clinical assessment by clinicians.

SARS-CoV-2 whole genome and phylogenetic analysis

Adapter sequences and reads of low-quality bases (Q20 < 10) and shorter than 40 bp were removed by fastp²⁶. High-quality reads were aligned to the reference genome of SARS-CoV-2 (GenBank: MN908947.3) utilizing the Burrows-Wheeler Aligner (BWA)²⁷. Reads with high mapping quality over 25 were reserved using SAMtools²⁸. A mutant allele was designated if its frequency was ≥ 0.7 , while a degenerate nucleotide was assigned if the mutant allele frequency ranging 0.3 to 0.7; otherwise, the reference allele was assigned. Variants with a minor allele frequency (MAF) > 0.3 and their impacts on genes, transcripts, protein sequences, and regulatory regions were annotated using the ensemble variant effect predictor (VEP)^{29,30}. Sequencing depth and genome coverage were calculated based on high-quality mapped (HQM) reads without duplications. SARS-CoV-2 genomes were analyzed using the Nextclade tool (<https://clades.nextstrain.org>) for multiple alignment and phylogenetic tree construction³¹. SARS-CoV-2 lineage was followed Pango lineage with PUSHES-v 1.19 database³². Tree visualization was carried out using iTOL³³.

Clinical data collection

Clinical characteristics, physical examination data, medications and treatments of COVID-19 patients were extracted from admission and discharged records. Severe pneumonia was assessed by clinical physicians according to multiple scoring systems, including CURB-65³⁴, Pneumonia Severity Index (PSI)³⁵, CURXO³⁶ and SMART-COP³⁷. Patients were divided into two groups according to the presence or absence of severe pneumonia. There were 69 cases in the severe pneumonia group and 131 cases in the non-severe pneumonia group. Radiological images were reviewed by qualified physicians. White blood cell (WBC), neutrophil and lymphocyte counts were collected from the reports closest to the sampling time of the mNGS specimen involved and no more than a week. The study was approved by the Ethics Committee of Ruijin Hospital in accordance with the Helsinki Declaration.

Statistics

Continuous variables not normally distributed are presented as medians (interquartile range [IQR]), while categorical variables are described as counts (%). Blood cell counts were analysed using the mean and corresponding 95% confidence interval (95% CI). The Wilcoxon signed-rank test and the Mann–Whitney U test were used for comparative analysis, as appropriate. The chi-square test (χ^2) was employed to assess distributions across different groups. The Hosmer–Lemeshow test was performed in the unconditional logistic regression analysis, where the variables were selected by back-ward procedure. Graphs were created using GraphPad Prism version 8.4.0 software. Venn diagrams were generated with jvenn, an interactive Venn diagram viewer. Statistical analyses were conducted using SPSS version 27.0 software, and a two-sided p-value of <0.05 was considered statistically significant.

Results

Pango lineage of SARS-CoV-2 variants

Reliable SARS-CoV-2 Pango lineages were available from mNGS data for 122 (61%) patients, with sufficient reads of SARS-CoV-2 covering 96.30 to 99.89% of the genome (median reads: 29,420 [13,973–47,422] vs. 612.5 [119.3–2,300], $p < 0.0001$) (Fig. S1). The most prevalent sub-lineages were FU.1 (20.5%), EG.5.1.1 (17.2%), FY.3 (11.5%), and XBB.1.16.1 (11.5%), accounting for more than half of the cases (Fig. 2a). Over time, XBB.1.16 was the most frequently detected sub-lineage from May to June, but then gradually decreased, while FU.1 was consistently detected during this period, and HK.3 began to emerge in August and increased steadily (Fig. 2b). When we compared the frequency of these sub-lineages in the severe group and the non-severe group (Fig. 2c),

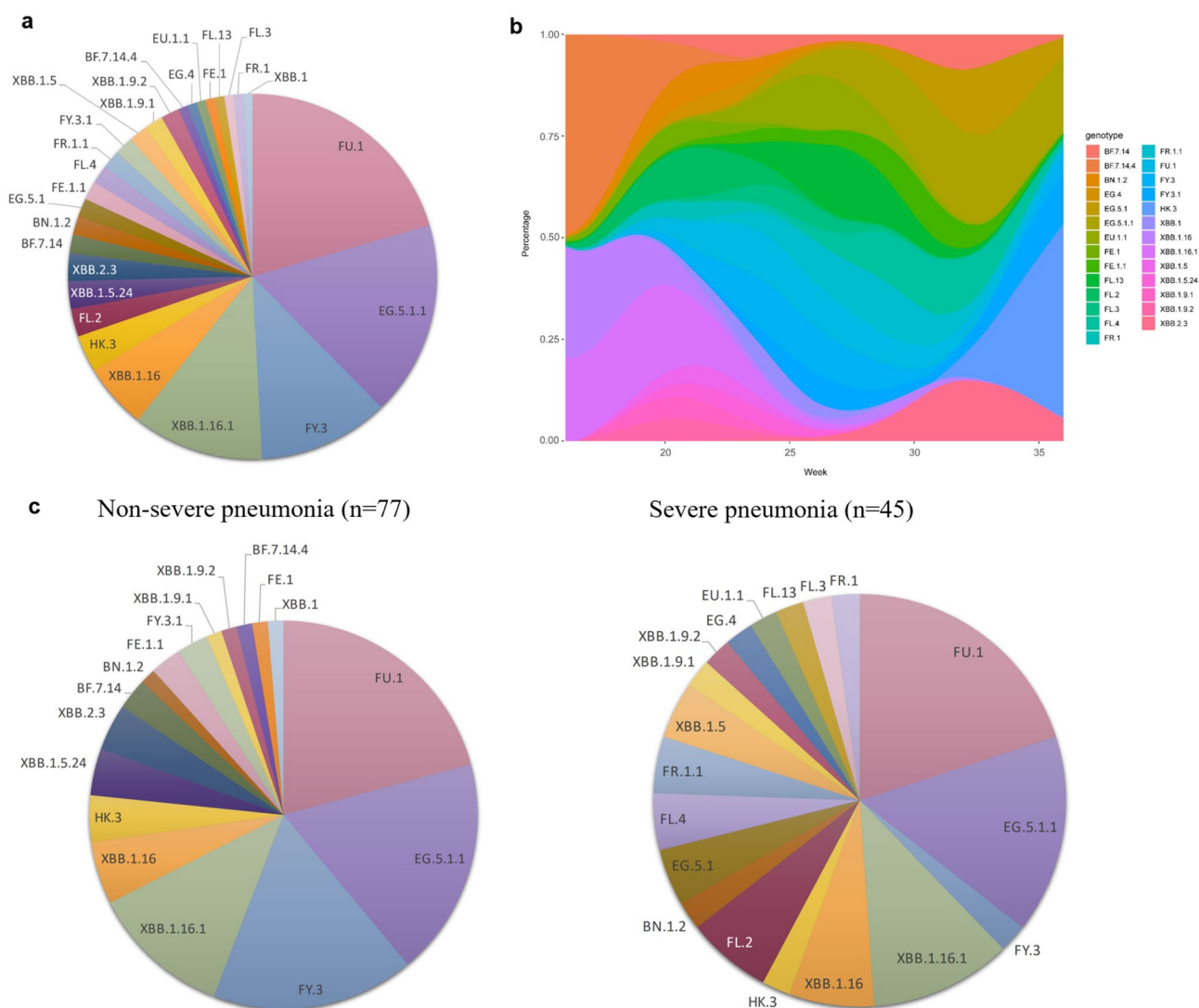


Fig. 2. Distribution and relative frequencies of SARS-CoV-2 sub-lineages from March to September, 2023. (a) The proportion of different Pango lineages available in 122 patients. (b) the weekly relative frequencies of SARS-CoV-2 sub-lineages over time. The week numbers started from the first week of 2023. (c) The proportion of different Pango lineages available in severe and non-severe pneumonia patients.

we found no significant differences in the distribution of lineages between the two groups (Table 1). Eleven patients exhibited blood viremia (Supplementary Table 1). Subvariants EG.5.1, FR.1, FL.2, and FU.1 were identified in severe cases, while XBB.1.16 and XBB.2.3 were detected in non-severe cases. Since phylogenetic analysis indicated minimal variation in the evolutionary branches of Omicron variants from April to September 2023 (Fig. 3), no significant association was observed between SARS-CoV-2 sub-lineages and either viremia occurrence or disease severity (Supplementary Table 1 and Supplementary Table 2). Although no specific lineage predominated in COVID-19 patients, the proportions of different sub-lineages fluctuated monthly.

Co-detected pathogens by mNGS

Co-infection patterns were analysed by categorizing pathogens into bacteria, fungi, and viruses, excluding torque teno virus (TTV). A total of 143, 117 and 132 samples of patients tested positive for bacteria, fungi and viruses alongside SARS-CoV-2 (Fig. 4a). A total of 185 patients (92.50%) developed co-infections of varying patterns, as shown in (Fig. 4b). The bacteria-fungi-virus co-infection was the most common combination in the non-severe pneumonia group (42.7%), while bacteria-fungi (21.7%) and bacteria-fungi-virus (21.7%) co-infections had similar proportions in the severe pneumonia group. There was no significant difference in the proportion of co-infection pattern between the two groups. We further analysed the pathogens that were most likely to be detected alongside SARS-CoV-2. The top five bacteria were *Enterococcus faecalis* (32/200, 16.00%), *Acinetobacter baumannii* (29/200, 14.50%), *Klebsiella pneumoniae* (24/200, 12.00%), *Stenotrophomonas maltophilia* (20/200, 10.00%), and *Staphylococcus aureus* (20/200, 10.00%) (Fig. 5a). Among fungi, *Candida albicans* (73/200, 36.50%), *Candida glabrata* (21/200, 10.50%), *Aspergillus fumigatus* (20/200, 10.00%), *Candida tropicalis* (18/200, 9.00%), and *Pneumocystis jirovecii* (18/200, 9.00%) were the most detected (Fig. 5b). As for virus, Epstein-Barr virus (EBV) (82/200, 41.00%), Human herpesvirus-7 (HHV-7) (63/200, 31.5%), Herpes simplex virus-1 (HSV-1) (31/200, 15.5%), Cytomegalovirus (CMV) (21/200, 10.5%) and Human herpesvirus-6 (HHV-6) (5/200, 2.50%) were widely detected among the patients (Fig. 5c). In addition to these herpesviruses with potential pathogenic significance, the other co-detected virus included Rhinovirus A and C (RV-A, RV-C), Human coronavirus-OC43 (HCoV-OC43), Human metapneumovirus (HMPV), and Human respiratory syncytial virus B (HRSV-B) (Fig. 5d).

Clinical characteristics and risk factor analysis of severe-pneumonia in COVID-19 patients

The demographic and clinical characteristics were presented in (Table 2). Severe pneumonia was identified in 69 (34.5%) patients, of whom 55 were male (79.71%), with a median age of 74 years (65.5–79 years). There were more elderly patients (aged > 65) in the severe pneumonia group compared with the non-severe group ($p = 0.014$), with 80 cases (61.07%) and 54 cases (78.26%), respectively. Common comorbidities included hypertension (102, 51%), malignancies (90, 45%), obesity (BMI > 25, 86, 43%), and diabetes mellitus (62, 31%). Significant differences were observed between the two groups in terms of hypertension (59, 45.04 vs 43, 62.32%), diabetes mellitus (31, 23.66 vs 31, 44.93%), chronic kidney disease (13, 9.92 vs 15, 21.74%), and chemotherapy (40, 30.53 vs 9, 13.04%) ($p < 0.05$).

Age over 65 years old and comorbidities such as hypertension, diabetes mellitus and chronic kidney disease were correlated with severe-pneumonia in all 200 COVID-19 patients by univariate logistic regression, while gender and the other comorbidities were not associated. In multivariate analysis, only the diabetes mellitus was statistically significant, which could be an independent risk factor of severe pneumonia (Table 3).

Fever and cough were the most frequently reported symptoms, affecting 132 (66%) and 117 (58.5%) patients, respectively. Fever (78, 59.54% vs 54, 78.26%) and shortness of breath (25, 19.08% vs 33, 47.83%) showed significant differences between the two groups ($p = 0.0079$ and $p < 0.0001$, respectively). Radiological findings revealed higher rates of patchy/ground-glass opacities (60, 86.96%), pulmonary exudation (25, 36.23%), and pleural effusion (34, 49.27%) in the severe pneumonia group, while pulmonary nodules were more common in the non-severe group (79, 60.31%). Decreased lymphocyte count, a typical feature of COVID-19, was more frequently observed in the severe pneumonia group (74, 56.48 vs. 63, 91.30%, $p < 0.0001$). Additionally, systolic blood pressure and respiratory rate differed significantly between the two groups ($p < 0.05$ for both). Thirty-five patients were hospitalized for underlying diseases, such as rheumatologic disorders, of which 32 patients were in the non-severe pneumonia group.

Treatments and outcomes of COVID-19 patients

Commonly used treatment drugs included PAXLOVID, LAGEVRIO, VV116, and Azvudine, and there was no significant difference in medication regimen between patients with severe and non-severe pneumonia ($p = 0.1266$) (Table 4). PAXLOVID was the most frequently used drug (96, 48%). Mask or nasal cannula oxygen therapy (107, 53.5%) was the most common way of oxygen supply, while mechanical ventilation (invasive: 11,

Sub-lineages	Non-severe pneumonia (n = 77)	Severe pneumonia (n = 45)	Total	p
FU.1	16 (20.78%)	9 (20.00%)	25 (20.50%)	0.0931
EG.5.1.1	14 (18.18%)	7 (15.56%)	21 (17.21)	
FY.3	13 (16.89%)	1 (2.22%)	14 (11.48%)	
XBB.1.16.1	9 (11.69%)	5 (11.11%)	14 (11.48%)	
Others	25 (32.47%)	23 (51.11%)	48 (39.34%)	

Table 1. Sub-lineages of SARS-CoV-2 in 122 COVID-19 patients.

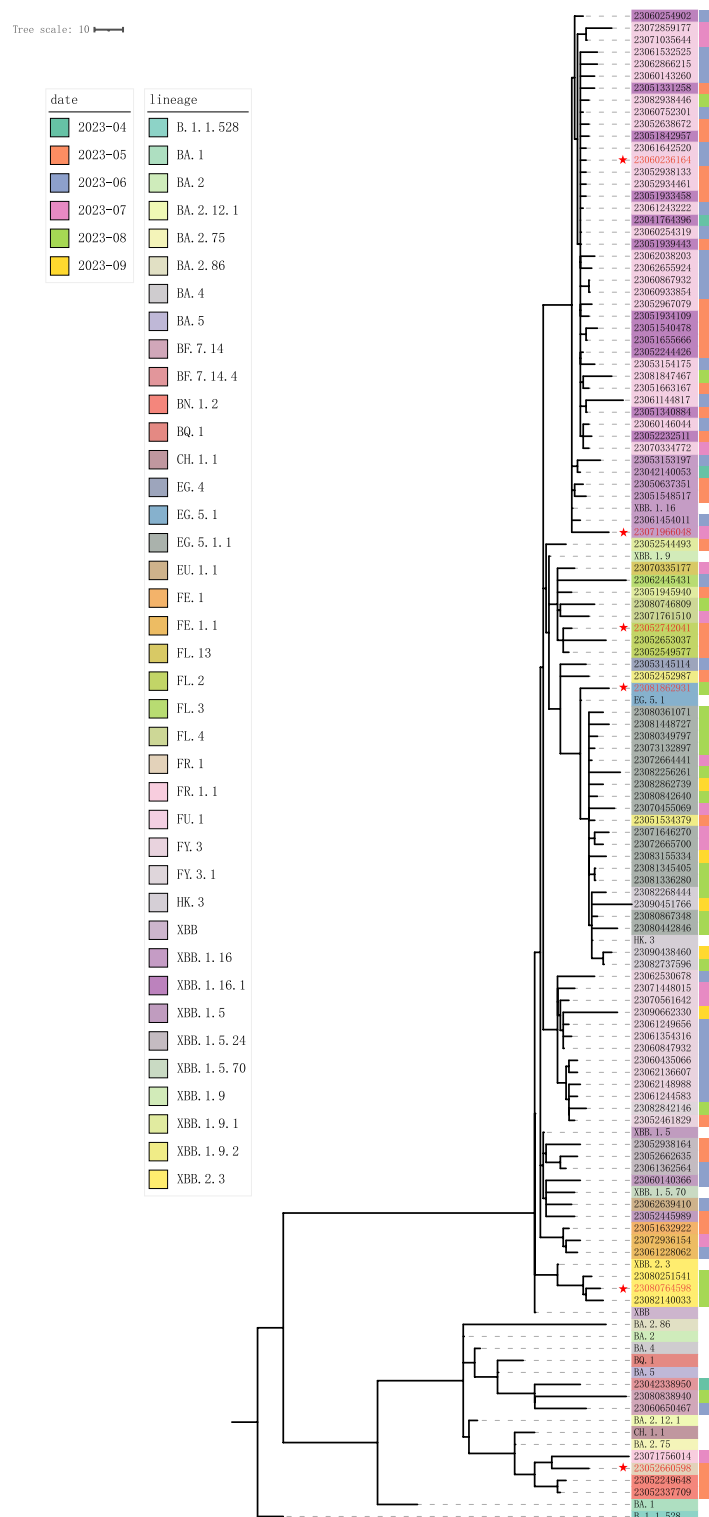


Fig. 3. Phylogenetic analysis of SARS-CoV-2 lineages and clinical correlates. The amino acid sequences were converted from nucleotide sequences using MEGA-X (10.1.8). Phylogenetic construction was performed by IQ-TREE (1.6.12). The GTR + F model was used for nucleotide sequences, while the Blosom62 model was used for amino acid sequences. Maximum-likelihood phylogenetic tree (scale bar: 10 nucleotide substitutions per site) reconstructed from SARS-CoV-2 genomic sequences, highlighting lineages circulating between April and September 2023. Red stars (*) denote six viral isolates from patients with confirmed viremia, mapped to specific branches of the Omicron subvariants. Lineage nomenclature follows PANGO classification, with temporal distribution of dominant variants annotated monthly. The detection of viremia-associated strains across phylogenetically distinct clusters underscores the need for genotype-agnostic monitoring of systemic infection risks.

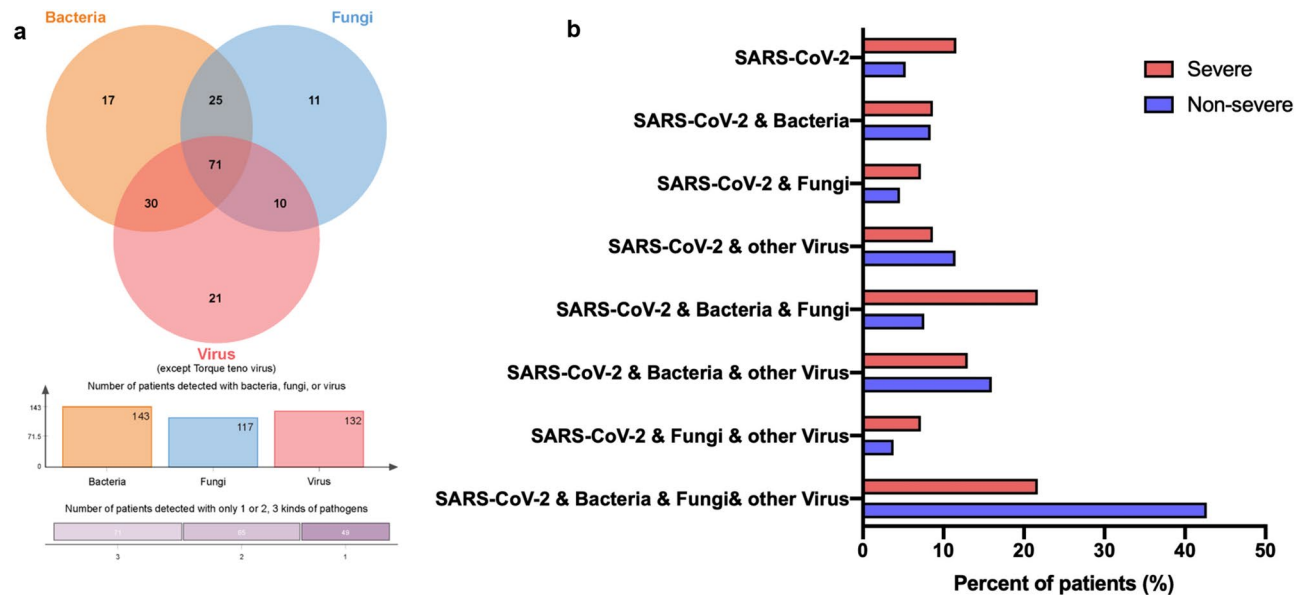


Fig. 4. Co-infection patterns with SARS-CoV-2. **(a)** Venn diagrams of pathogens co-detected with SARS-CoV-2. Numbers on the diagram indicate the number of patients who tested positive for bacteria, fungi, or virus. Torque teno virus was excluded. **(b)** Co-infection patterns of severe and non-severe pneumonia in COVID-19 patients.

15.94%, and non-invasive: 6, 8.70%) was more frequently used in the severe pneumonia group. One patient in the non-severe group received extracorporeal membrane oxygenation (ECMO) following cardiac surgery. As for the outcomes of these patients, all deaths occurred in the severe pneumonia group.

Discussion

mNGS is an efficient diagnostic tool because it is high-throughput and has the potential to provide early, actionable diagnoses³⁸. In this study, we retrospectively analysed the variation of SARS-CoV-2 detected by mNGS over approximately six months, as well as the characteristics of co-pathogens and the clinical features of the corresponding patients. Phylogenetic analysis revealed minimal divergence among SARS-CoV-2 sub-lineages, with continuous evolutionary fluctuations mirroring epidemic dynamics. No significant association was observed between SARS-CoV-2 sub-lineages and pneumonia severity. However, severe pneumonia cases predominantly occurred in elderly patients with complex underlying comorbidities. This approach is critical for both tracking Omicron subvariant evolution and identifying co-pathogens in high-risk populations such as immunocompromised cohorts.

Since the COVID-19 outbreak in December 2019, SARS-CoV-2 variants have attracted continuous attention. Several waves of the global pandemic have been driven by SARS-CoV-2 variants of concern (VOCs), such as Omicron, which is currently the most prevalent strain⁶. The evolution of these variants remains a key area of research³⁹. By late November 2021, Omicron BA.1 had rapidly displaced the prior VOC Delta with Omicron associated with lower severity and mortality⁴⁰. According to China national center for bioinformatics (CNCB) from 1st March to 31st August 2023, a total of 9236 SARS-CoV-2 sequences were uploaded in Shanghai, of which EG.5.1.1 variant was accounted for 22.01%, FU.1 accounted for 20.54%. The Omicron sub-lineages identified in our study demonstrated concordance with national surveillance data. Despite demonstrating attenuated pathogenicity and lacking lineage-specific severity correlations (Supplementary Table 2), Omicron subvariants still caused severe pneumonia in high-risk populations, highlighting the importance of developing broad-spectrum immunity through vaccination strategies targeting multiple subvariants.

SARS-CoV-2 is typically easier to be detected in respiratory tract specimens, such as nasopharyngeal swabs, bronchoalveolar lavage fluid, and sputum. However, we detected SARS-CoV-2 sequences in the blood samples of four patients included in our analysis, as well as in an additional seven blood samples from different patients with respiratory tract specimens already collected (Supplementary Table 1). Seven of these patients were diagnosed with severe pneumonia. Although specific subvariants were identified in these cases, no significant association was observed between viral sub-lineages and viremia occurrence. The development of viremia appeared more closely associated with patients' underlying comorbidities and immunosuppressed status. In the previous study, SARS-CoV-2 viral loads, particularly plasma viremia, have been associated with an increased risk of mortality⁴¹. Additionally, host immunosuppression can result in increased viral shedding and altered SARS-CoV-2 viral decay kinetics^{42,43}. Given the medical history of these patients in our study, the presence of SARS-CoV-2 sequences in the blood of severe pneumonia patients may be due to lung tissue damage, which could allow the release of viral nucleic acid into the bloodstream. In patients with malignant tumours and severe immunosuppression following

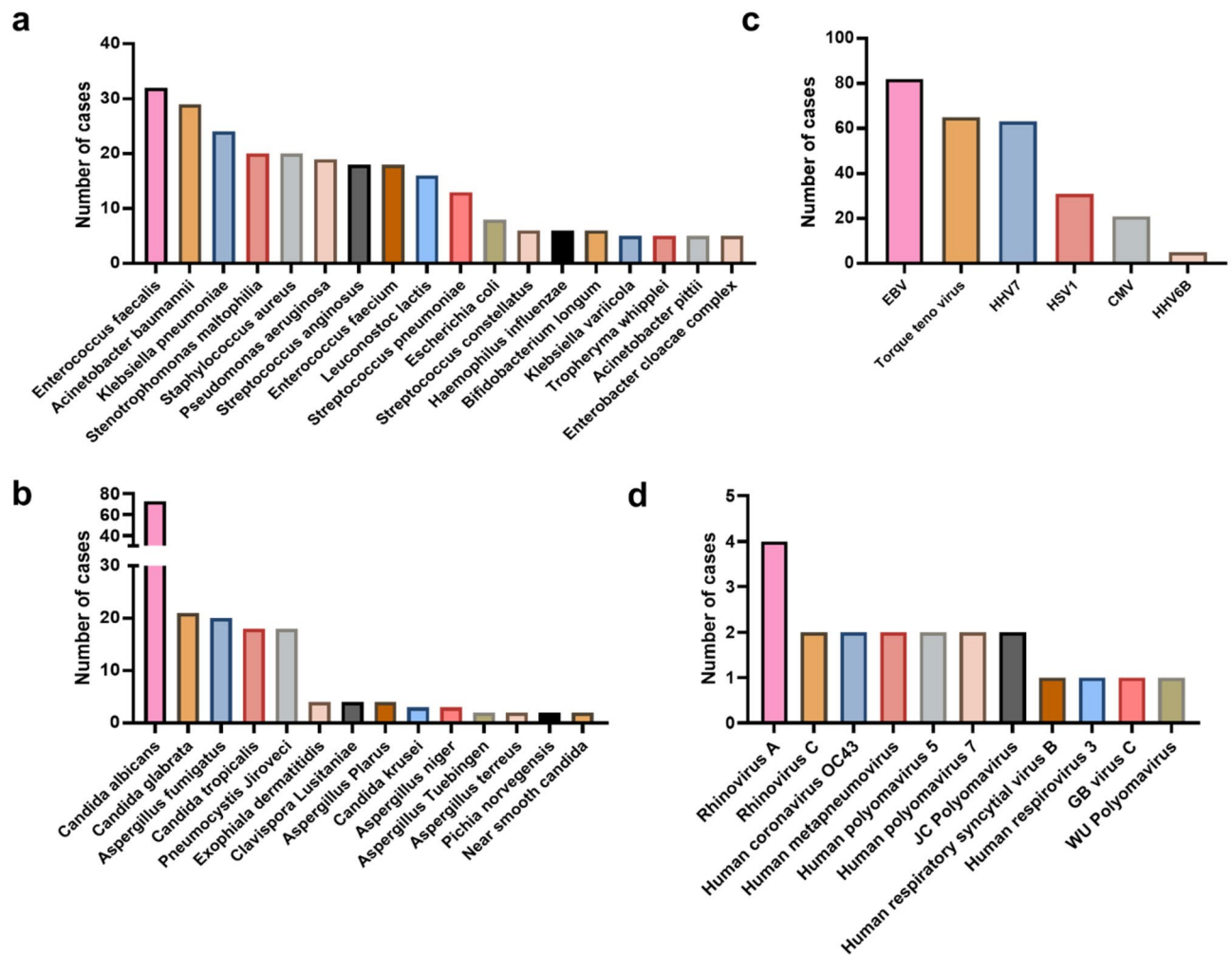


Fig. 5. Frequency of each pathogen co-detected alongside SARS-CoV-2. **(a)** Bacteria co-detected with SARS-CoV-2. **(b)** Fungi co-detected with SARS-CoV-2. **(c)** Viruses co-detected with SARS-CoV-2 exclude Torque teno virus. **(d)** Viruses co-detected with SARS-CoV-2 exclude Torque teno virus and herpesviruses.

chemoradiation, the inability to control viral spread may also lead to viremia. Therefore, blood RNAemia could serve as a critical marker for disease severity, especially in immunosuppressed patients^{44,45}.

Co-infection and secondary infection remain major challenges in the treatment of COVID-19 pneumonia. Meanwhile, mNGS may have more superiority in diagnosis of mixed infections, especially for intensive care unit (ICU) patients⁴⁶. Although mNGS demonstrated significantly higher pathogen detection rates compared to conventional microbiological methods, distinguishing microbial colonization from infection cannot be determined solely by mNGS results^{14,15}. We analysed pathogens that were confirmed to have clinical relevance by evaluating characteristics of clinical profiles and assessments of clinicians, despite their possible colonization potential. Previously, bacterial infections commonly occur in patients with prolonged hospital stays, with *Pseudomonas aeruginosa*, *Klebsiella* spp., and *Staphylococcus aureus* being the most frequent pathogens⁴⁷. Additionally, the mechanisms underlying susceptibility to invasive fungal infections following respiratory viral infections are complex⁴⁸. COVID-19-associated invasive fungal infections, such as those caused by *Aspergillus*, *Mucorales*, and *Candida* species, are a significant complication in critically ill, hospitalized patients⁴⁹. Although the other pathogens and SARS-CoV-2 cannot be strictly distinguished as a first infected pathogen because some patients were admission for their underlying diseases, similar bacterial and fungal co-infection patterns were still observed, and broad-spectrum antibacterial and antifungal agents were used in hospitalized patients. Additionally, potential co-infections with Herpesviridae were frequently detected in COVID-19 patients. A meta-analysis of active EBV, CMV, HSV, Varicella Zoster virus (VZV), and HHV-6 infections in the COVID-19 population showed that one pathogen's activity can trigger the virulence of another⁵⁰. However, it was also difficult to distinguish by mNGS whether these Herpesviridae were active. After excluding viruses with potential pathogenicity, we still detected other pathogenic viruses alongside SARS-CoV-2. Co-infection with rhinovirus, respiratory syncytial virus, or other respiratory tract viruses occurred easily, which significantly increased the odds of requiring invasive mechanical ventilation and in-hospital mortality⁵¹. Similarly, a systematic analysis found that patients with viral co-infections were more likely to experience dyspnoea and had a higher mortality

		Non-severe pneumonia (n = 131)	Severe pneumonia (n = 69)	P
Gender	Male	88 (67.18%)	55 (79.71%)	0.0619
	Female	43 (32.82%)	14 (20.29%)	
Age	Median (years)	68 (58 ~ 78)	74 (65.5 ~ 79)	0.0277
	< 65	51 (38.93%)	15 (21.74%)	0.014
	≥ 65	80 (61.07%)	54 (78.26%)	
Comorbidity	Hypertension	59 (45.04%)	43 (62.32%)	0.0201
	Obesity	57 (43.51%)	29 (42.03%)	0.8405
	Malignancies	64 (48.85%)	26 (37.68%)	0.1311
	Chemotherapy	40 (30.53%)	9 (13.04%)	0.0063
	Diabetes mellitus	31 (23.66%)	31 (44.93%)	0.0002
	Cardiovascular disease	29 (22.14%)	18 (26.09%)	0.5312
	Chronic cardiac disease	23 (17.56%)	17 (26.64%)	0.234
	Chronic pulmonary disease	19 (14.5%)	12 (17.39%)	0.5917
	Chronic kidney disease	13 (9.92%)	15 (21.74%)	0.0221
	Liver disease	13 (9.92%)	9 (13.04%)	0.5027
	Rheumatologic disorder	11 (8.4%)	6 (8.7%)	0.9426
	Malnutrition	6 (4.58%)	8 (11.59%)	0.1196
	Smoking	7 (5.35%)	1 (1.45%)	0.3388
	Chronic neurological disorder	4 (3.05%)	4 (5.80%)	0.5743
	Chronic haematological disease	3 (2.29%)	1 (1.45%)	1.0000
	Tuberculosis	3 (2.29%)	1 (1.45%)	1.0000
	Dementia	1 (0.76%)	1 (1.45%)	1.0000
Symptom	Fever	78 (59.54%)	54 (78.26%)	0.0079
	Cough	72 (54.96%)	45 (65.22%)	0.1617
	Expectoration	54 (41.22%)	33 (47.83%)	0.3704
	Shortness of breath	25 (19.08%)	33 (47.83%)	< 0.0001
	Fatigue/malaise	10 (7.63%)	7 (10.14%)	0.5449
	Muscle aches/joint pain	9 (6.87%)	5 (7.25%)	1.0000
	Vomiting/nausea	12 (9.16%)	3 (4.35%)	0.2193
	Headache	7 (5.34%)	5 (7.25%)	0.8261
	Pulmonary shadow	6 (4.58%)	0 (0%)	0.0952
	Diarrhoea	3 (2.29%)	2 (2.9%)	1.0000
	Abdominal pain	1 (0.76%)	2 (2.9%)	0.2739
	Altered consciousness/confusion	1 (0.76%)	2 (2.9%)	0.2739
Radiology	Pleural effusion	23 (17.56%)	34 (49.28%)	< 0.0001
	Exudation	14 (10.69%)	25 (36.23%)	< 0.0001
	Patchy/ground-glass opacity	85 (64.89%)	60 (86.96%)	0.0009
	Pulmonary nodule	79 (60.31%)	23 (33.33%)	0.0003
Complete blood count	Leukocyte (10 ⁹ /L)	7.16 (6.43 to 7.90)	9.69 (8.19 to 11.19)	0.0033
	Neutrophil (10 ⁹ /L)	5.41 (4.67 to 6.18)	8.65 (7.26 to 10.04)	< 0.0001
	Lymphocyte (10 ⁹ /L)	1.61 (0.61 to 2.61)	0.611 (0.38 to 0.84)	0.0550
Physical examination	Heart rate	87.47 (84.29 to 90.64)	91.36 (87.27 to 95.45)	0.1451
	Systolic blood pressure	125.40 (121.80 to 128.90)	139.80 (133.70 to 145.90)	< 0.0001
	Diastolic blood pressure	73.93 (71.73 to 76.13)	76.99 (74.33 to 79.64)	0.0931
	Respiratory rate	19.60 (19.19 to 20.02)	21.28 (20.04 to 22.51)	0.0123

Table 2. Demographic and clinical characteristics of COVID-19 patients.

rate (OR 1.66)⁵². There was no significant difference in co-infection patterns between the severe and non-severe groups in our study, which was likely because these non-severe pneumonia patients also had highly complicated underlying conditions, often involving severe immunosuppression.

It is obvious that the elderly COVID-19 patients require more attention in clinical treatment, especially those with underlying diseases. In this study, severe cases were predominantly observed in older patients, especially those over 65 years of age. Most young and middle-aged patients experienced mild or asymptomatic infections, while greater attention should be given to the elderly, particularly those with underlying conditions. A retrospective observational cohort study in Italy, conducted from March 2020 to June 2022, revealed that 34.7% of patients had severe COVID-19, with the highest mortality rates occurring in older adults across all waves⁵³. Similarly, a retrospective study in Spain found that advanced age and comorbidities were associated

Parameter	Univariate analysis		Multivariate analysis	
	OR (95%CI) ^a	P value	OR (95%CI) ^a	P value
Age				
< 65	Reference value			
> = 65	2.295 (1.173, 4.491)	0.015	1.721 (0.813, 3.643)	0.156
Gender				
Male	Reference value			
Female	1.920 (0.926, 3.830)	0.064		
Comorbidity				
Hypertension	2.018 (1.112, 3.664)	0.021	1.184 (0.591, 2.370)	0.634
Obesity	0.941 (0.522, 1.698)	0.840		
Malignancies	0.633 (0.349, 1.148)	0.132		
Chemotherapy	0.341 (0.154, 0.754)	0.341		
Diabetes mellitus	2.632 (1.412, 4.904)	0.002	2.033 (1.029, 4.015)	0.041
Cardiovascular disease	1.241 (0.631, 2.444)	0.532		
Chronic cardiac disease	1.535 (0.756, 3.119)	0.236		
Chronic pulmonary disease	1.241 (0.563, 2.734)	0.592		
Chronic kidney disease	2.521 (1.122, 5.665)	0.025	2.226 (0.948, 5.224)	0.066
Liver disease	1.362 (0.551, 3.365)	0.504		
Rheumatologic disorder	1.039 (0.367, 2.941)	0.943		
Malnutrition	2.731 (0.908, 8.224)	0.074		
Smoking	0.261 (0.031, 2.162)	0.213		
Chronic neurological disorder	1.954 (0.473, 8.065)	0.354		
Chronic haematological disease	0.627 (0.064, 6.148)	0.689		
Tuberculosis	0.627 (0.064, 6.148)	0.689		
Dementia	1.912 (0.118, 31.041)	0.649		

Table 3. Logistic regression analysis of factors associated with severe-pneumonia of COVID-19 patients. ^aOR odds ratio, CI confidence interval.

		Non-severe pneumonia (n = 131)	Severe pneumonia (n = 69)	P
Anti-SARS-CoV-2 agent	PAXLOVID	56 (42.75%)	23 (33.33%)	0.1266
	LAGEVRIO	27 (20.61%)	22 (31.88%)	
	VV116	15 (11.45%)	2 (2.90%)	
	Azvudine	3 (2.29%)	2 (2.90%)	
	PAXLOVID + LAGEVRIO	5 (3.82%)	7 (10.14%)	
	PAXLOVID + VV116	1 (0.76%)	2 (2.90%)	
	LAGEVRIO + VV116	1 (0.76%)	0 (0.00%)	
	PAXLOVID + LAGEVRIO + VV116	1 (0.76%)	1 (1.45%)	
	Non	22 (16.79%)	10 (14.49%)	
Oxygen supplementation	Extracorporeal membrane oxygenation	1 (0.76%)	1 (1.45%)	< 0.0001
	Invasive mechanical ventilation ¹	2 (1.53%)	11 (15.94%)	
	Non-invasive mechanical ventilation ²	1 (0.76%)	6 (8.70%)	
	Oxygen therapy via mask or nasal cannula	64 (48.85%)	43 (62.32%)	
	In room air	63 (48.09%)	7 (10.14%)	
Outcome	Discharge	128 (97.71%)	46 (66.67%)	< 0.0001
	Death	0 (0.00%)	23 (33.33%)	
	Still in hospital	3 (2.29%)	0 (0.00%)	

Table 4. Anti-SARS-CoV-2 treatment of COVID-19 patients and outcomes. ¹Invasive mechanical ventilation requires endotracheal intubation or tracheostomy to deliver positive pressure ventilation for patients with respiratory failure. ²Non-invasive ventilation provides positive pressure support via facial or nasal interfaces for patients with moderate to severe respiratory insufficiency.

with increased hospital mortality⁵⁴. An international cohort study of COVID-19 patients, spanning 52 countries between January 2020 and January 2022, reported that age was the strongest predictor of mortality risk; each comorbidity nearly doubled the risk of death. Additionally, smoking and obesity were linked to higher mortality risks⁵⁵. Although the patients enrolled in our study were admitted with complex underlying diseases, these risk factors were noted in our cohort, despite only diabetes mellitus was statistically significant (Table 3).

Conclusion

The bioinformatic analysis of mNGS showed that SARS-CoV-2 infection still occurred commonly in hospitalized patients, perhaps causing severe pneumonia in patients with underlying diseases such as diabetes mellitus. SARS-CoV-2 lineages showed slight distance in the evolutionary branches and no significant evidence in the severity of pneumonia. Potential pathogens detected by mNGS may lead to complex infections, obliging early intervention. The diagnostic capability of mNGS in detecting coinfections makes it particularly valuable for determining causative pathogens in cases of undetermined etiology.

Strengths and limitations

The application of metagenomic next-generation sequencing (mNGS) in clinical laboratories facilitated the analysis of co-infective pathogens, a task that was challenging for conventional laboratory methods. It provided more complete infection patterns of COVID-19 patients, especially the individuals with complex underlying conditions. The findings of this study have to be seen in light of two limitations. First, mNGS was not a routine laboratory examination and was recommended only for patients with complex conditions; as a result, data on mild cases were limited in our study. Secondly, the outcomes of these patients were more significantly influenced by underlying diseases, particularly malignancies and immunosuppression. In the future, we would conduct more bioinformatics analysis and to explore the application of mNGS in more infection styles.

Data availability

Sequence data that support the findings of this study have been deposited in the SRA database of National Center for Biotechnology Information with the primary accession code PRJNA1241481. Our SRA records will be accessible with the following link after the indicated release date: <https://www.ncbi.nlm.nih.gov/sra/PRJNA1241481>.

Received: 22 March 2025; Accepted: 26 May 2025

Published online: 29 May 2025

References

1. Liu, D. et al. Multicenter assessment of shotgun metagenomics for pathogen detection. *EBioMedicine* **74**, 103649 (2021).
2. Diao, Z. et al. Validation of a metagenomic next-generation sequencing assay for lower respiratory pathogen detection. *Microbiol. Spectr.* **11** (1), e0381222 (2023).
3. Deng, X. et al. Metagenomic sequencing with spiked primer enrichment for viral diagnostics and genomic surveillance. *Nat. Microbiol.* **5** (3), 443–454 (2020).
4. Chen, L. et al. RNA based mNGS approach identifies a novel human coronavirus from two individual pneumonia cases in 2019 Wuhan outbreak. *Emerg. Microbes Infect.* **9** (1), 313–319 (2020).
5. Carbo, E. C. et al. A comparison of five illumina, ion torrent, and nanopore sequencing technology-based approaches for whole genome sequencing of SARS-CoV-2. *Eur. J. Clin. Microbiol. Infect. Dis.* **42** (6), 701–713 (2023).
6. Wei, D. et al. Pathogen evolution, prevention/control strategy and clinical features of COVID-19: experiences from China. *Front. Med.* **17** (6), 1030–1046 (2023).
7. Wei, D. et al. Sequential reinfection with Omicron variants elicits broader neutralizing antibody profiles in booster vaccinees and reduces the duration of viral shedding. *J. Med. Virol.* **95** (10), e29151 (2023).
8. Cao, Y. et al. BA.2.12.1, BA.4 and BA.5 escape antibodies elicited by omicron infection. *Nature* **608** (7923), 593–602 (2022).
9. Krause, P. R. et al. SARS-CoV-2 variants and vaccines. *N. Engl. J. Med.* **385** (2), 179–186 (2021).
10. Suleiman, A. S. et al. A meta-meta-analysis of co-infection, secondary infections, and antimicrobial resistance in COVID-19 patients. *J. Infect. Public Health* **16** (10), 1562–1590 (2023).
11. Miao, Q. et al. Microbiological diagnostic performance of metagenomic next-generation sequencing when applied to clinical practice. *Clin. Infect. Dis.* **67** (2), S231–S240 (2018).
12. Lin, T. et al. Microbiological diagnostic performance of metagenomic next-generation sequencing compared with conventional culture for patients with community-acquired pneumonia. *Front. Cell Infect. Microbiol.* **13**, 1136588 (2023).
13. Qu, J. et al. Aetiology of severe community acquired pneumonia in adults identified by combined detection methods: a multi-centre prospective study in China. *Emerg. Microbes Infect.* **11** (1), 556–566 (2022).
14. Lv, M. et al. Clinical values of metagenomic next-generation sequencing in patients with severe pneumonia: a systematic review and meta-analysis. *Front. Cell Infect. Microbiol.* **13**, 1106859 (2023).
15. Liu, M. et al. The etiological diagnostic value of metagenomic next-generation sequencing in suspected community-acquired pneumonia. *BMC Infect. Dis.* **24** (1), 626 (2024).
16. Amar, Y. et al. Pre-digest of unprotected DNA by benzonase improves the representation of living skin bacteria and efficiently depletes host DNA. *Microbiome* **9** (1), 123 (2021).
17. Wang, C. et al. Toward efficient and high-fidelity metagenomic data from sub-nanogram DNA: evaluation of library preparation and decontamination methods. *BMC Biol.* **20** (1), 225 (2022).
18. Chen, H. et al. Clinical utility of in-house metagenomic next-generation sequencing for the diagnosis of lower respiratory tract infections and analysis of the host immune response. *Clin. Infect. Dis.* **71** (4), S416–S426 (2020).
19. Metsky, H. C. et al. Capturing sequence diversity in metagenomes with comprehensive and scalable probe design. *Nat. Biotechnol.* **37** (2), 160–168 (2019).
20. Liu, Y. et al. Diagnostic value of metagenomic next-generation sequencing of lower respiratory tract specimen for the diagnosis of suspected *Pneumocystis jirovecii* pneumonia. *Ann. Med.* **55** (1), 2232358 (2023).
21. Xu, Y. et al. Dynamics of severe acute respiratory syndrome coronavirus 2 genome variants in the feces during convalescence. *J. Genet. Genom.* **47** (10), 610–617 (2020).
22. Bolger, A. M., Lohse, M. & Usadel, B. Trimmomatic: a flexible trimmer for Illumina sequence data. *Bioinformatics* **30** (15), 2114–2120 (2014).

23. Li, H. & Durbin, R. Fast and accurate short read alignment with Burrows-Wheeler transform. *Bioinformatics* **25** (14), 1754–1760 (2009).
24. Fiorini, N., Lipman, D. J. & Lu, Z. Towards PubMed 2.0. *Elife* **6**, e28801 (2017).
25. Miller, S. et al. Laboratory validation of a clinical metagenomic sequencing assay for pathogen detection in cerebrospinal fluid. *Genome Res.* **29** (5), 831–842 (2019).
26. Chen, S., Zhou, Y., Chen, Y. & Gu, J. fastp: an ultra-fast all-in-one FASTQ preprocessor. *Bioinformatics* **34** (17), i884–i890 (2018).
27. Jung, Y. & Han, D. BWA-MEME: BWA-MEM emulated with a machine learning approach. *Bioinformatics* **38** (9), 2404–2413 (2022).
28. Li, H. et al. The sequence alignment/map format and SAMtools. *Bioinformatics* **25** (16), 2078–2079 (2009).
29. Ma, W. et al. Genomic perspectives on the emerging SARS-CoV-2 omicron variant. *Genom. Proteom. Bioinformat.* **20** (1), 60–69 (2022).
30. McLaren, W. et al. The ensembl variant effect predictor. *Genome Biol.* **17** (1), 122 (2016).
31. Colson, P. et al. Role of SARS-CoV-2 mutations in the evolution of the COVID-19 pandemic. *J. Infect.* **88** (5), 106150 (2024).
32. O'Toole, A., Pybus, O. G., Abram, M. E., Kelly, E. J. & Rambaut, A. Pango lineage designation and assignment using SARS-CoV-2 spike gene nucleotide sequences. *BMC Genom.* **23** (1), 121 (2022).
33. Letunic, I. & Bork, P. Interactive Tree Of Life (iTOL) v5: an online tool for phylogenetic tree display and annotation. *Nucleic Acids Res.* **49** (W1), W293–W296 (2021).
34. Lim, W. S. et al. Defining community acquired pneumonia severity on presentation to hospital: an international derivation and validation study. *Thorax* **58** (5), 377–382 (2003).
35. Fine, M. J. et al. A prediction rule to identify low-risk patients with community-acquired pneumonia. *N. Engl. J. Med.* **336** (4), 243–250 (1997).
36. España, P. P. et al. Development and validation of a clinical prediction rule for severe community-acquired pneumonia. *Am. J. Respir. Crit. Care Med.* **174** (11), 1249–1256 (2006).
37. Charles, P. G. P. et al. SMART-COP: a tool for predicting the need for intensive respiratory or vasopressor support in community-acquired pneumonia. *Clin. Infect. Dis.* **47** (3), 375–384 (2008).
38. Hogan, C. A. et al. Clinical impact of metagenomic next-generation sequencing of plasma cell-free DNA for the diagnosis of infectious diseases: A multicenter retrospective cohort study. *Clin. Infect. Dis.* **72** (2), 239–245 (2021).
39. Guan, M., Sun, N. & Yau, S. S. T. Geometric analysis of SARS-CoV-2 variants. *Gene* **909**, 148291 (2024).
40. Ali, K. M. et al. Clinical outcomes and phylogenetic analysis in reflection with three predominant clades of SARS-CoV-2 variants. *Eur. J. Clin. Invest.* **53** (9), e14004 (2023).
41. Fajnzylber, J. et al. SARS-CoV-2 viral load is associated with increased disease severity and mortality. *Nat. Commun.* **11** (1), 5493 (2020).
42. Li, Y. et al. Immune status and SARS-CoV-2 viral dynamics. *J. Infect. Dis.* **228** (2), S111–S116 (2023).
43. Roy-Vallejo, E. et al. SARS-CoV-2 viremia precedes an IL6 response in severe COVID-19 patients: Results of a longitudinal prospective cohort. *Front. Med.* **9**, 855639 (2022).
44. Lawrence Panchali, M. J. et al. SARS-CoV-2 RNAemia and disease severity in COVID-19 patients. *Viruses* **15** (7), 1560 (2023).
45. Giacomelli, A. et al. SARS-CoV-2 viremia and COVID-19 mortality: A prospective observational study. *PLoS ONE* **18** (4), e0281052 (2023).
46. Zhou, J. J. et al. Diagnostic value of metagenomic next-generation sequencing for pulmonary infection in intensive care unit and non-intensive care unit patients. *Front. Cell. Infect. Microbiol.* **12**, 929856 (2022).
47. Westblade, L. F., Simon, M. S. & Satlin, M. J. Bacterial coinfections in coronavirus disease 2019. *Trends Microbiol.* **29** (10), 930–941 (2021).
48. Salazar, F., Bignell, E., Brown, G. D., Cook, P. C. & Warris, A. Pathogenesis of respiratory viral and fungal coinfections. *Clin. Microbiol. Rev.* **35** (1), e0009421 (2022).
49. Hoenigl, M. et al. COVID-19-associated fungal infections. *Nat. Microbiol.* **7** (8), 1127–1140 (2022).
50. Banko, A., Miljanovic, D. & Cirkovic, A. Systematic review with meta-analysis of active herpesvirus infections in patients with COVID-19: Old players on the new field. *Int. J. Infect. Dis.* **130**, 108–125 (2023).
51. Swets, M. C. et al. SARS-CoV-2 co-infection with influenza viruses, respiratory syncytial virus, or adenoviruses. *Lancet* **399** (10334), 1463–1464 (2022).
52. Krumbein, H. et al. Respiratory viral co-infections in patients with COVID-19 and associated outcomes: A systematic review and meta-analysis. *Rev. Med. Virol.* **33** (1), e2365 (2023).
53. Trecarichi, E. M. et al. Evolution of in-hospital patient characteristics and predictors of death in the COVID-19 pandemic across four waves: are they moving targets with implications for patient care? *Front. Public Health* **11**, 1280835 (2023).
54. Peláez, A. et al. Clinical characteristics and outcomes among hospitalised COVID-19 patients across epidemic waves in Spain: An unCoVer analysis. *Med. Clin.* **162**, 523–531 (2024).
55. Kartsonaki, C. et al. Characteristics and outcomes of an international cohort of 600 000 hospitalized patients with COVID-19. *Int. J. Epidemiol.* **52** (2), 355–376 (2023).

Acknowledgements

This study was funded by Shanghai Municipal Science and Technology Major Project (ZD2021CY001), National Key Research and Development Program of China (2024YFC3044400) and Shanghai Targeted Biomedical Emergency Project (23DX1900300). We thank all the participants involved in this study.

Author contributions

X.Z., M.Z., J.M., J.L. and L.H. had the idea for and designed the study. X.L., X.Y. and C.T. were responsible for collecting and summarizing the clinical data. X.L. and X.Y. performed the experimental studies. X.L. and X.Y. carried out the analysis. X.L. and C.T. drafted the manuscript. X.Z. revised the manuscript. All authors reviewed and approved the final version.

Funding

This study was funded by Shanghai Municipal Science and Technology Major Project (ZD2021CY001), National Key Research and Development Program of China (2024YFC3044400) and Shanghai Targeted Biomedical Emergency Project (23DX1900300). We thank all the participants involved in this study.

Declarations

Competing interests

The authors declare no competing interests.

Ethics approval and consent to participate

The study was approved by the Ethics Committee of Ruijin Hospital in accordance with the Helsinki Declaration. The Review Board exempted requirement for informed consent since this retrospective study used only the laboratory samples and did not have any negative impact on the patients.

Additional information

Supplementary Information The online version contains supplementary material available at <https://doi.org/10.1038/s41598-025-04111-3>.

Correspondence and requests for materials should be addressed to X.Y. or X.Z.

Reprints and permissions information is available at www.nature.com/reprints.

Publisher's note Springer Nature remains neutral with regard to jurisdictional claims in published maps and institutional affiliations.

Open Access This article is licensed under a Creative Commons Attribution-NonCommercial-NoDerivatives 4.0 International License, which permits any non-commercial use, sharing, distribution and reproduction in any medium or format, as long as you give appropriate credit to the original author(s) and the source, provide a link to the Creative Commons licence, and indicate if you modified the licensed material. You do not have permission under this licence to share adapted material derived from this article or parts of it. The images or other third party material in this article are included in the article's Creative Commons licence, unless indicated otherwise in a credit line to the material. If material is not included in the article's Creative Commons licence and your intended use is not permitted by statutory regulation or exceeds the permitted use, you will need to obtain permission directly from the copyright holder. To view a copy of this licence, visit <http://creativecommons.org/licenses/by-nc-nd/4.0/>.

© The Author(s) 2025